Eur Radiol
DOI 10.1007/s00330-017-4899-4

NEURO

The diagnostic value of high-frequency power-based diffusion-weighted imaging in prediction of neuroepithelial tumour grading

Zhiye Chen[1,2] · Peng Zhou[3,4] · Bin Lv[5] · Mengqi Liu[1,2] · Yan Wang[1] · Yulin Wang[1] · Xin Lou[1] · Qiuping Gui[6] · Huiguang He[3,4,7] · Lin Ma[1]

Received: 21 March 2017 / Revised: 23 April 2017 / Accepted: 16 May 2017

Abstract

Objectives To retrospectively evaluate the diagnostic value of high-frequency power (HFP) compared with the minimum apparent diffusion coefficient (MinADC) in the prediction of neuroepithelial tumour grading.

Methods Diffusion-weighted imaging (DWI) data were acquired on 115 patients by a 3.0-T MRI system, which included b0 images and b1000 images over the whole brain in each patient. The HFP values and MinADC values were calculated by an in-house script written on the MATLAB platform.

Results There was a significant difference among each group excluding grade I (G1) vs. grade II (G2) ($P = 0.309$) for HFP and among each group for MinADC. ROC analysis showed a higher discriminative accuracy between low-grade glioma (LGG) and high-grade glioma (HGG) for HFP with area under the curve (AUC) value 1 compared with that for MinADC with AUC 0.83 ± 0.04 and also demonstrated a higher discriminative ability among the G1-grade IV (G4) group for HFP compared with that for MinADC except G1 vs. G2.

Conclusions HFP could provide a simple and effective optimal tool for the prediction of neuroepithelial tumour grading based on diffusion-weighted images in routine clinical practice.

Key Points

- *HFP shows positive correlation with neuroepithelial tumour grading.*
- *HFP presents a good diagnostic efficacy for LGG and HGG.*
- *HFP is helpful in the selection of brain tumour boundary.*

Keywords Diffusion-weighted imaging · High-frequency power · Minimum apparent diffusion coefficient · Neuroepithelial tumour grading · Magnetic resonance imaging

Electronic supplementary material The online version of this article (doi:10.1007/s00330-017-4899-4) contains supplementary material, which is available to authorized users.

✉ Huiguang He
huiguang.he@ia.ac.cn

✉ Lin Ma
cjr.malin@vip.163.com

1 Department of Radiology, Chinese PLA General Hospital, Fuxing Road 28, Beijing 100853, China

2 Department of Radiology, Hainan Branch of Chinese PLA General Hospital, Sanya 572013, China

3 Research Center for Brain-inspired Intelligence, Institute of Automation, Chinese Academy of Sciences, Beijing 100190, China

4 University of Chinese Academy of Sciences , Beijing 100190, China

5 Academy of Telecommunication Research of MIIT, Beijing 100083, China

6 Department of Pathology, Chinese PLA General Hospital, Beijing 100853, China

7 Center for Excellence in Brain Science and Intelligence Technology, Chinese Academy of Sciences, Beijing 100190, China

Abbreviations

AUC	Area under the curve
DWI	Diffusion-weighted imaging
G1	Grade I
G2	Grade II
G3	Grade III
G4	Grade IV
HFP	High-frequency power
HGG	High-grade glioma
LGG	Low-grade glioma
MinADC	Minimum apparent diffusion coefficient
ROC	Receiver-operating characteristics curve

Published online: 12 June 2017

Introduction

Neuroepithelial tumours are the most common primary tumours of the central nervous system, and tumour grading was related with the biological behaviour and prognosis [1]. Common brain tumour grading methods include a magnetic resonance imaging (MRI) enhancement examination [2–4], magnetic resonance spectroscopy (MRS) [5, 6], perfusion-weighted imaging (PWI) [4, 7, 8], susceptibility-weighted imaging (SWI) [9], chemical exchange saturation transfer (CEST) [10], three-dimensional pseudo-continuous arterial spin labelling (3D-ASL) [7], and positron emission tomography (PET) [11, 12]. These techniques are all advanced examinations and may require a long scan time, contrast administration, and specific MR sequence, which are not routinely carried out. Sometimes, the patient is intolerant of the long time of the examination or contrast enhancement.

Diffusion-weighted imaging (DWI) is a simple practicable MR technique that can detect the microscopic motion of the water molecule. In our previous study, the minimum ADC (MinADC) was used to evaluate the neuroepithelial tumour grading [13]; however, its main limitation was the MinADC value overlap between the LGG and the HGG. In addition, ADC computation involved b0 (b value = 0 s/mm^2) and b1000 images (b value = 1000 s/mm^2), and visual assessment was only based on the b1000 images; herein, ADC value assessment was not accordant with the visual assessment.

High-frequency power (HFP) parameter values reflect the abrupt jump in signal intensity from the normal to pathological region (boundary region). The HFP parameter values can be assessed and possibly used in grading the different stages of the haemorrhage based on DWI [14]. Up to now, it was not used for the assessment of neuroepithelial tumour grading.

The DWI signal variance in the lesion reflects the tumour cell heterogeneity, and the transitional zones surrounding the tumour boundary may really reflect the tumour development and the invasive characteristics. The aim of this study is to investigate the HFP changes on the transitional zones (tumour boundary) based on the DWI (b value = 1000 s/mm^2 but not the ADC map) and compare the diagnostic value of HFP and MinADC in the prediction of neuroepithelial tumour grading.

Methods

Participants

This study received prior approval from our Institutional Review Board and Ethics Committee, and written informed consent was not required since DWI scans are routinely performed in clinical practice in our hospital. One hundred fifteen consecutive patients (69 males, 46 females; 5-85 years, mean age 43.01 ± 15.60 years) were included in the present study, including 76 astrocytic tumours, 20 oligodendroglial tumours, 11 oligoastrocytic tumours, and 8 ependymal tumours. Medical records, MR data, surgical records, and pathological reports were available in all cases.

MRI acquisition

All MR images were acquired on a 3.0-T whole-body MR imaging system (Signa EXCITE, GE Healthcare, Milwaukee, WI, USA) with a conventional eight-channel phased-array head coil. The conventional MR scan included the pre-contrast T1-weighted image (T1WI), T2-weighted image (T2WI), DWI, and post-contrast T1WI. DWI was performed using a fat-suppressed single-shot spin-echo echo-planar imaging (TR/TE = 6000 ms/65.7 ms, slice thickness = 6.0 mm, slice space = 1.0 mm, field of view = 24 × 24 cm, matrix = 192 × 192, NEX = 2) with b = 1000 s/mm^2 applied in the x, y, and z directions and b = 0 s/mm^2 without motion-probing gradients, followed by automatic generation of the DWI. All the patients received navigation-guided operations within 3 days after MR examination. Intraoperative MRI was used to define the brain shift because of the craniotomy and CSF leaking out and to correct the navigation plan before the surgical resection.

Data processing

DWI images were used for the study. The HFP and ADC values of each voxel were calculated by an in-house script written on MATLAB (The MathWorks, Inc., Natick, MA, USA) platform. The data processing is described in the supplemental materials.

The rectangle ROI (37-132 mm^2) was manually drawn on the boundary between the tumour and the surrounding brain tissue with the centre on the boundary in the range of the biopsy before surgical resection by an experienced neuroradiologist who was blinded to patient identity and pathological diagnosis and grading (Fig. 1). The ROI should have the highest contrast between the tumour and the surrounding brain tissue, avoiding the cystic, necrotic regions, especially haemorrhagic regions in the tumour, which may influence HFP measurement [14]. Intra-rater reliability of the HFP value and MinADC value was also assessed. The same rater outlined the ROIs in the 115 patients at least 2 months later according the previous ROI records and selected slice records. Mean HFP and MinADC values were regarded as the final HFP and MinADC value.

Pathological observation

All the patients received stereotactic biopsy before surgical resection. The biopsy and the removed specimens were fixed in formalin and embedded with paraffin. Haematoxylin and eosin-stained specimens and immunohistochemical analysis were performed to determine the histological type of the

tumour after surgery. All the biopsy pathological grading was consistent with the final pathological grading. The procedure was performed by an experienced pathologist. According to WHO criteria [15], WHO I (G1) and II(G2) were classified as the low-grade glioma (LGG) group while WHO III (G3) and IV(G4) as the high-grade glioma group (HGG).

Statistical analysis

The data were presented as mean ± standard deviation. The intraclass correlation coefficient calculated by using a one-way random model was used to test the intra-rater reproducibility. The statistical significance was calculated using one-way analysis of variance (ANOVA) with Dunnett's T3 method because of unequal variances of HFP and the least significant difference (LSD) because of equal variances of MinADC among G1 ~ G4 and subtypes of neuroepithelial tumours. HPF and MinADC values between LGG and HGG groups were analysed with the Welch test because of variance non-homogeneity. Spearman's correlation analysis was performed between pathological grading and the HFP and MinADC value.

Receiver-operating characteristic curve (ROC) analysis was applied to assess the best cut-off value of the HFP and MinADC. The area under the ROC curve (AUC) was used to assess the diagnostic ability of the HFP and MinADC value.

Significant difference was set at a P value less than 0.05. The statistical analysis was performed with IBM SPSS Statistics for MS Windows (SPSS Inc., Chicago, IL, USA), release 19.

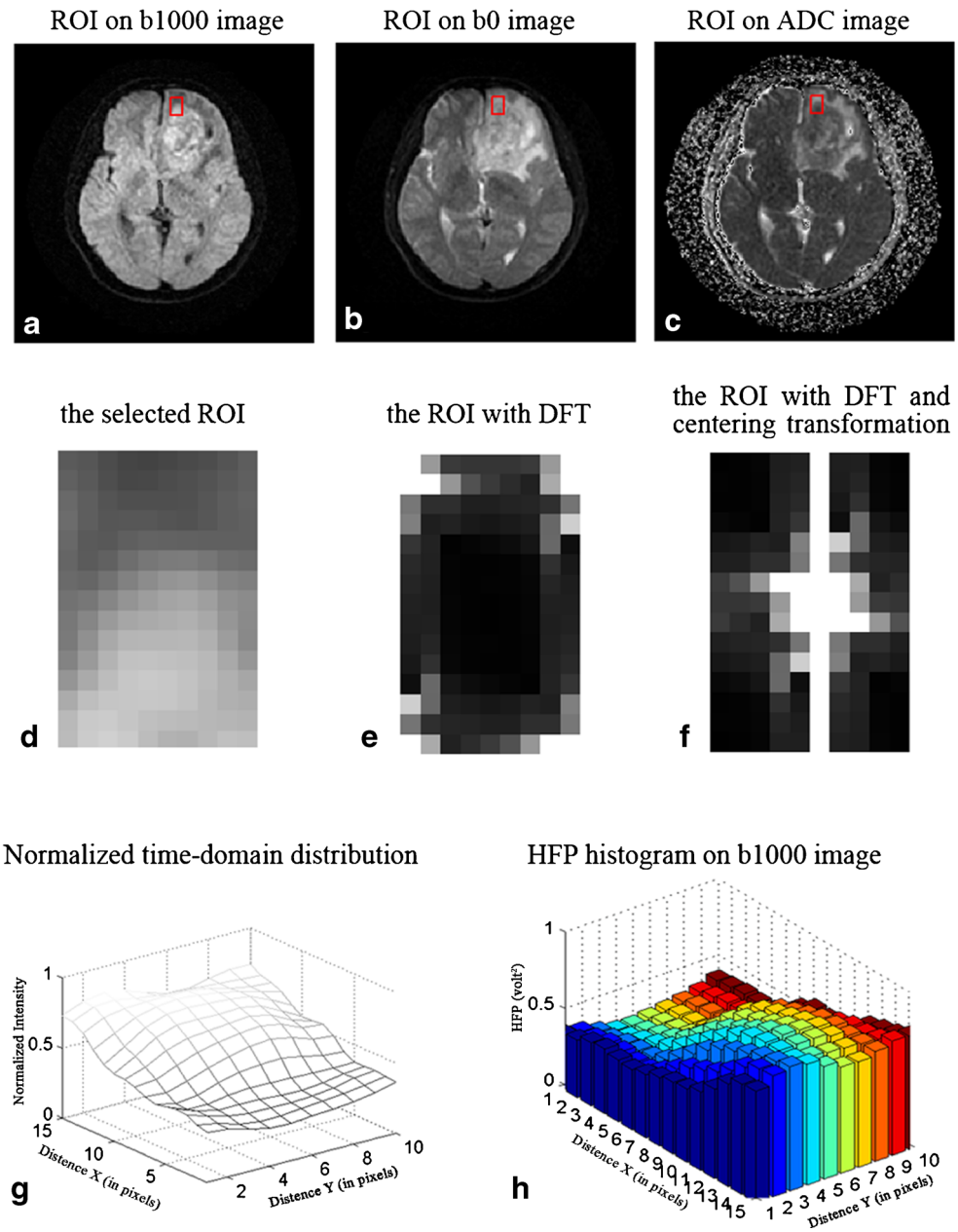

Fig. 1 HFP measurement on diffusion-weighted images. **a** The ROI manually drawn on the b1000 image; **b** the corresponding ROI automatically selected on the b0 image; **c** the corresponding ROI automatically selected on the ADC image; **d** the selected ROI; **e** the ROI with discrete Fourier transform (DFT); **f** the ROI with DFT and centring transformation; **g** normalised time-domain distribution; **h** HFP histogram on the b1000 image

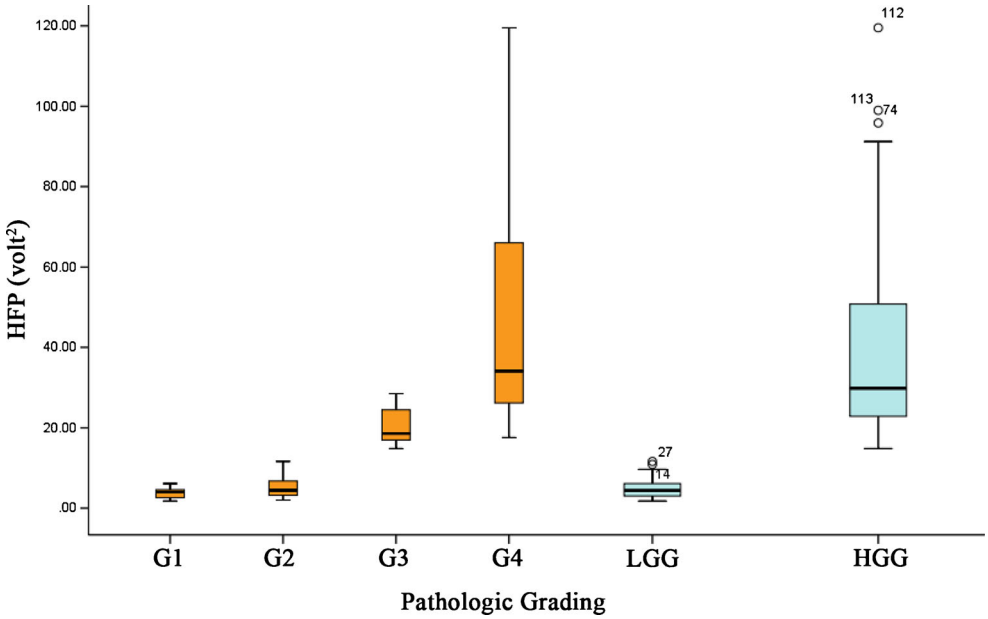

Fig. 2 The distribution graph of the HFP in the WHO grading and low and high neuroepithelial grading. LGG includes G1 and G2; HGG includes G3 and G4

Results

Pathological results

In 115 patients, the number of G1, G2, G3, and G4 was 9, 48, 13, and 45, respectively. For 76 astrocytic tumours, 26 cases were LGG, and 50 cases were HGG. Of 20 oligodendroglial tumours, 14 cases were LGG, and 6 cases were HGG. Eleven oligoastrocytic tumours were all LGG. For eight ependymal tumours, six cases were LGG, and two cases were HGG. Herein, the total number of LGG was 57 cases and HGG was 58 cases, respectively.

Comparison of the HFP and MinADC value among grading groups

The intraclass correlation coefficient (ICC) was 0.993 for HFP and 0.775 for MinADC. HFP values of G1, G2, G3, G4, LGG, and HGG were 3.86 ± 1.49 volt^2, 5.07 ± 2.48 volt^2, 20.62 ± 4.76 volt^2, 46.70 ± 26.01 volt^2, 4.88 ± 2.38 volt^2, and 40.08 ± 25.27 volt^2, respectively (Fig. 2). The MinADC value of G1, G2, G3, G4, LGG, and HGG was $0.95 \pm 0.12 \times 10^{-3}$mm^2/s, $0.76 \pm 0.12 \times 10^{-3}$mm^2/s, $0.68 \pm 0.08 \times 10^{-3}$mm^2/s, $0.61 \pm 0.10 \times 10^{-3}$mm^2/s, $0.79 \pm 0.14 \times 10^{-3}$mm^2/s, and $0.62 \pm 0.10 \times 10^{-3}$mm^2/s, respectively (Fig. 3).

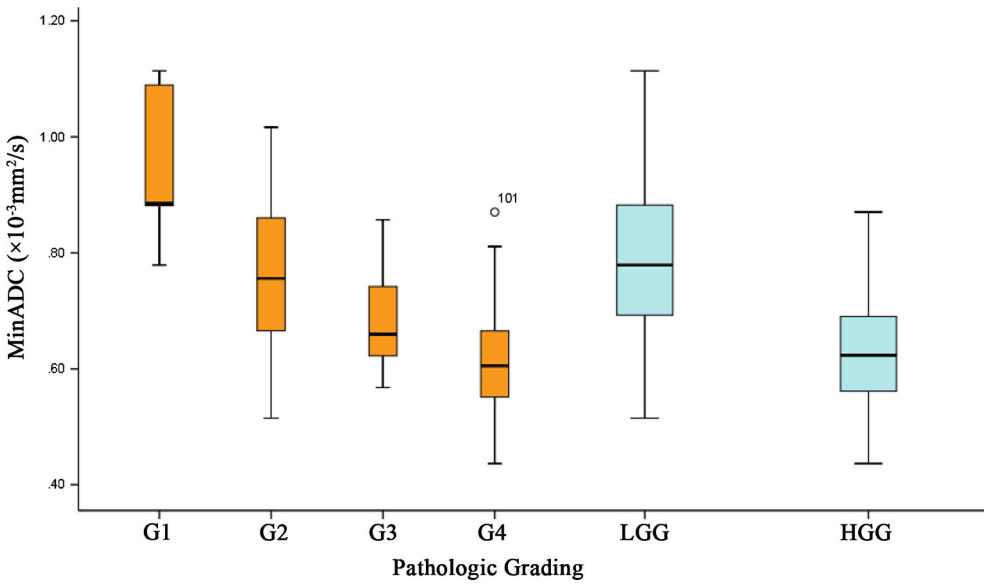

Fig. 3 The distribution graph of MinADC values in the WHO grading and low and high neuroepithelial grading. LGG includes G1 and G2; HGG includes G3 and G4

One-way ANOVA indicated that there was significant difference for HFP among each compared group ($P = 0.000$) except G1 vs. G2 ($P = 0.309$), and there was also evident difference for the MinADC value among each group ($P < 0.05$). HFP and MinADC values presented a significant difference between LGG and HGG by the Welch test ($P < 0.05$) (Table 1).

Figure 4 shows the signal intensity (time-domain) distribution on a patient with glioblastoma and a patient with low-grade astrocytoma. This indicated that the variance of signal intensity was evident in HGG compared to that in LGG based on the time-domain transformation, and the contralateral ROI (normal brain tissue) showed a minimal variance of signal intensity. These findings also confirmed that HGG had a high value of HFP components compared with LGG.

Table 1 Comparison of HFP and MinADC among G1-G4, LGG, and HGG

Group	HFP (*P* value)[a]	MinADC (*P* value)[b]
G1 vs. G2	0.309	0.000
G1 vs. G3	0.000	0.000
G1 vs. G4	0.000	0.000
G2 vs. G3	0.003	0.021
G2 vs. G4	0.000	0.000
G3 vs. G4	0.000	0.049
LGG vs. HGG[c]	0.000	0.000

[a] Comparisons of HFP among G1-G4 were analysed by using one-way ANOVA with Dunnett's T3 method because of unequal variances; [b] comparisons of MinADC among G1-G4 were analysed by using one-way ANOVA with the LSD method because of equal variances; [c] comparisons of HFP and MinADC between LGG and HGG were analysed by using the Welch test because of variance nonhomogeneity.

G1, WHO grade 1; G2, WHO grade 2; G3, WHO grade 3; G4, WHO grade 4; LGG, low-grade neuroepithelial tumour; HGG, high-grade neuroepithelial tumour; HFP, high-frequency power; MinADC, minimum apparent diffusion coefficient

Correlation analysis

Spearman's correlation analysis demonstrated that there was a significant positive correlation between pathological grading

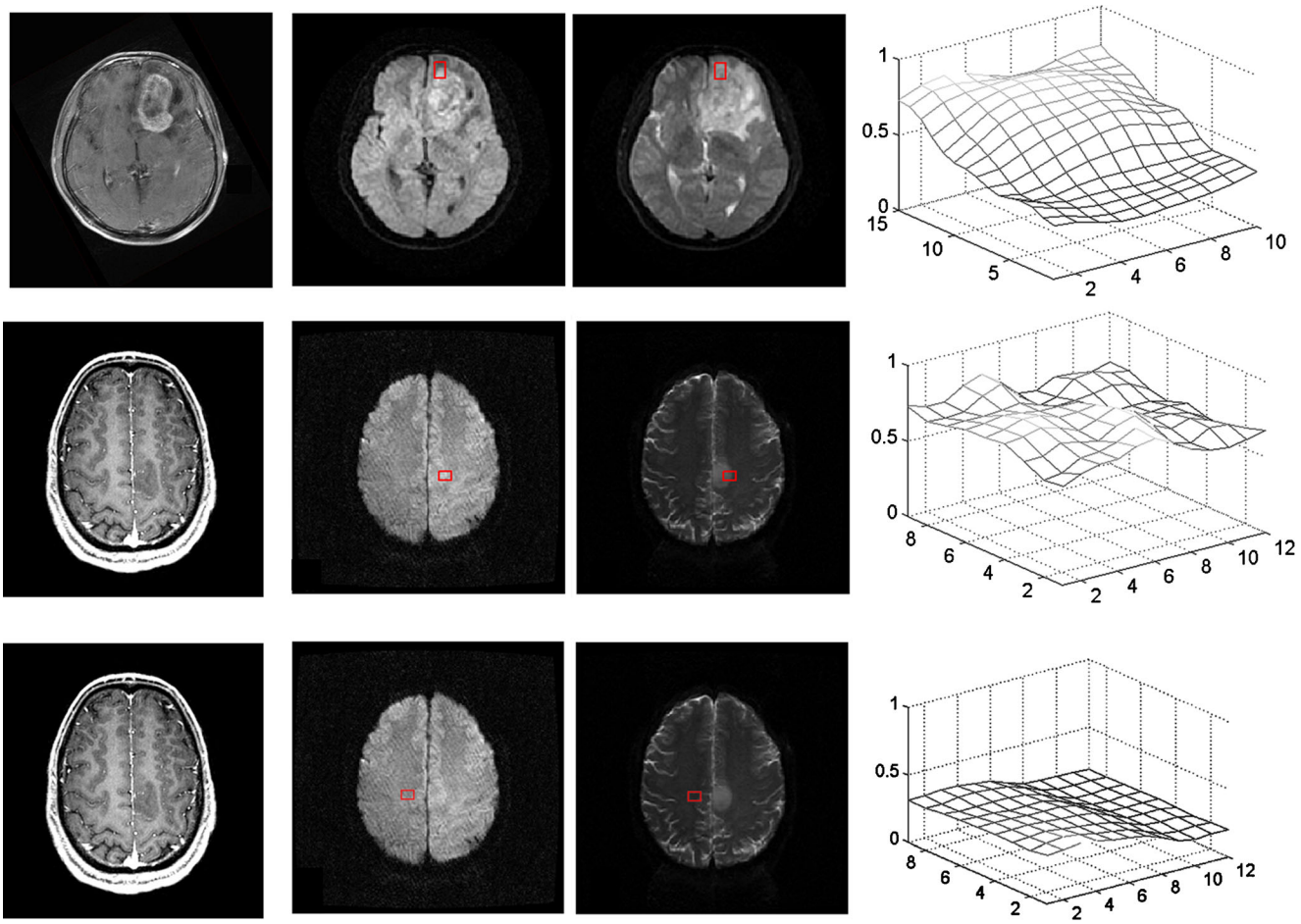

Fig. 4 Case image (b1000 images) intensity (time-domain) distribution. The *top line* was a 49-year-old male patient with glioblastoma (WHO IV); the *middle line* was a 53-year-old female patient with astrocytoma (WHO II), and the *bottom line* was the same as the middle line on the same patient. The ROI was placed in b1000 images (the *second column*), and the corresponding ROI was placed on the b0 image (the *third column*) automatically, and ROI signal intensity (time-domain) distribution plots (the *last column*) were generated. The ROI on the *bottom* was the mirrored ROI for the *middle line images*. The variance of signal intensity was more evident in HGG than that in LGG, and the contralateral ROI (normal brain tissue) showed a minimal variance in signal intensity. The *first column* was the contrast-enhanced T1WI

Table 2 ROC analysis of HFP and MinADC for discrimination among WHO neuroepithelial tumour grading

	HFP (volt^2)						MinADC ($\times 10^{-3}$ mm^2/s)					
	G1 vs. G2	G1 vs. G3	G1 vs. G4	G2 vs. G3	G2 vs. G4	G3 vs. G4	G1 vs. G2	G1 vs. G3	G1 vs. G4	G2 vs. G3	G2 vs. G4	G3 vs. G4
Cut-off value	6.24	10.49	11.87	13.24	14.62	28.61	0.86	0.77	0.78	0.74	0.66	0.57
AUC	0.63 ± 0.10	1.00	1.00	1.00	1.00	0.90 ± 0.04	0.85 ± 0.06	0.99 ± 0.01	0.99 ± 0.01	0.71 ± 0.07	0.82 ± 0.04	0.71 ± 0.07
Sensitivity	0.29	1.00	1.00	1.00	1.00	0.67	0.73	0.92	0.96	0.77	0.73	0.40
Specificity	1.00	1.00	1.00	1.00	1.00	1.00	0.89	1.00	1	0.60	0.81	1

G1, WHO grade 1; G2, WHO grade 2; G3, WHO grade 3; G4, WHO grade 4; LGG, low-grade neuroepithelial tumour; HGG, high-grade neuroepithelial tumour; HFP, high-frequency power; MinADC, minimum apparent diffusion coefficient; ROC, ROC, receiver-operating characteristic curve; AUC, area under the curve

and HFP ($r = 0.876$) ($P = 0.000$) and a significant negative correlation between pathological grading and the MinADC value ($r = -0.632$) ($P = 0.000$).

ROC analysis between LGG and HGG

ROC analysis between LGG and HGG showed that the AUC of HFP (AUC = 1) was larger than that of the MinADC value (AUC = 0.83 ± 0.04), and HFP had a higher sensitivity and specificity (100% and 100%) compared with that (67% and 84%) of the MinADC value. The cut-off value of the HFP and MinADC value was 13.24 volt^2 and 0.66×10^{-3}mm^2/s, respectively.

ROC analysis among G1 ~ G4

Table 2 indicates that there was a higher AUC for HFP compared with the MinADC value (Fig. 4) in G1 vs. G3, G1 vs. G4, G2 vs. G3, G2 vs. G4, and G3 vs. G4. However, there was a relatively low AUC (AUC = 0.63 ± 0.10) for HFP compared with that (AUC = 0.85 ± 0.06) of the MinADC value in G1 vs. G2.

Discussion

In the present study, it was demonstrated that the HFP had a high diagnostic value for LGG and HGG, and it showed no overlap in the tumour grading discrimination. It even showed a good judgement ability among G1 ~ G4 except G1 vs. G2. Compared with HFP, MinADC showed a low discriminant ability, and overlap existed when the tumour grading was performed. This overlap limited the clinical practice value of MinADC on the neuroepithelial tumour grading [13]. Further, Spearman's correlation analysis demonstrated that HFP had a relatively higher correlation with pathological grading than the MinADC value. The correlation level suggested that HFP was more sensitive in evaluating the neuroepithelial grading relative to MinADC (Fig. 4).

While quantitative analysis of HFP could provide accurate neuroepithelial tumour grading, the visual assessment could also present some important diagnostic information. Figure 1 shows that HGG commonly revealed significant variance of HFP compared with LGG and the normal brain tissue on the time-domain distribution plot, which indicated that HGG had abrupt jumps in spatial intensity variation and a high value of HFP components [14]. Thus, the time-domain distribution plot may be regarded as a valuable auxiliary diagnosis tool.

The ROC curve has been widely applied in the evaluation of radiological imaging and other medical imaging diagnostic tests [16–18], and it provides the most comprehensive description of diagnostic accuracy available to date. Its diagnostic accuracy is characterised by the combination of sensitivity and specificity, and its diagnostic efficacy can be assessed

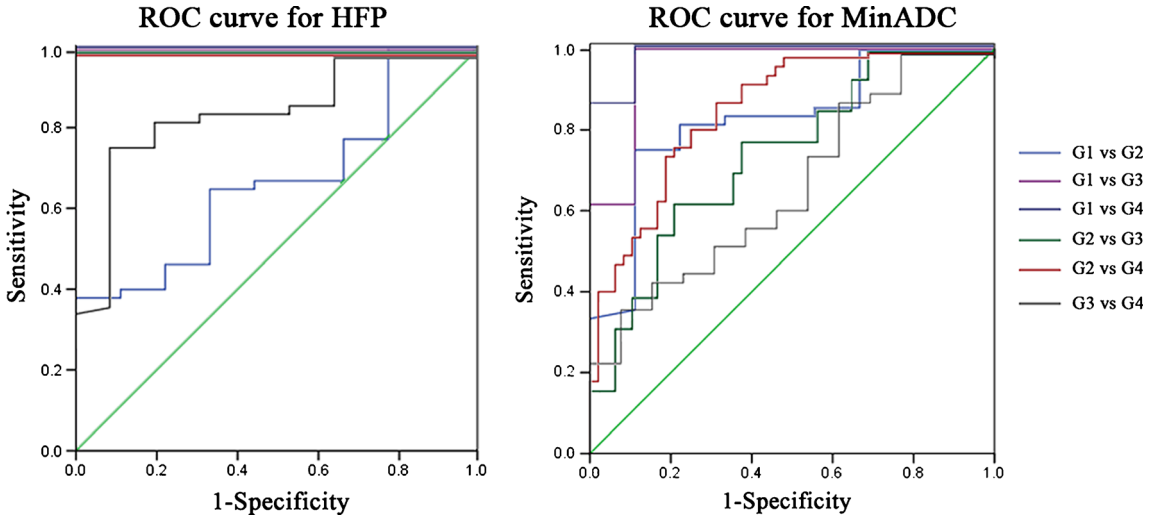

Fig. 5 ROC curves of HFP and MinADC discrimination between WHO neuroepithelial tumour gradings

by six levels [19]. In this study, ROC analysis demonstrated that HFP could totally distinguish LGG from HGG, and it had 100% sensitivity and specificity, while MinADC only had 67% sensitivity and 84% specificity and had a smaller AUC (AUC = 0.83 ± 0.04) compared with that (AUC = 1) of HFP. It also had an overlap between LGG and HGG (Fig. 5).

Although ROC suggested that HFP had a good diagnostic value for LGG vs. HGG and among G1 ~ G4 compared with the MinADC value, caution needed to be used when it was used to grade between G1 and G2 because it had a smaller AUC (AUC = 0.63 ± 0.10) and also had an overlap between G1 and G2 (Fig. 1). In contrast, MinADC showed no overlap between G1 and G2 (Fig. 2), and it had a good grading ability for G1 and G2 (AUC = 0.85 ± 0.06). However, care needed to be taken when it was used to distinguish G3 from G4 because of its small AUC (AUC = 0.71 ± 0.07), and the overlap was observed between G3 and G4 (Fig. 2).

In a previous study [20], the signal intensity gradient (SIG) method was applied with quantitative analysis of diffusion-weighted images to compare glioma with meningioma. With this technique, a tumour ROI and contralateral ROI with the same location and size were generated, and the SIG value of each subregion was evaluated by the Robinson compass operator comprising eight kernels. The highest SIGmax value was the subregion that exhibited the highest cellular density and was chosen as the resultant SIG value. Therefore, SIGmax would be similar to the MinADC value, which represents the highest tumour cellularity of the neuroepithelial tumours [13]. HFP is a technique based on frequency domain analysis, and it represents the abrupt jump in signal intensity from the tumour area to normal-appearing region. It reflects the dynamic changes from pathological to normal tissue, especially on the lesion boundary, while the SIG technique represents the highest tumour cellularity in the tumour region and is a static characteristic.

HFP analysis in this study may provide a new viewpoint for the definition of the true boundary of a brain tumour, which would make possible to excise the brain tumour totally. It can be presumed that the true boundary may be located in the region with no abrupt jump in signal intensity based on the HFP technique, and the time-domain distribution shows no significant change or minimal variance. However, this should still be confirmed by pathology, and this was a limitation of this study. Another limitation of this study was that perfusion-weighted imaging was not carried out in all cases, which may be compared with HFP methods in identifying the tumour boundary.

In conclusion, HFP analysis on diffusion-weighted images can demonstrate a higher discriminative accuracy for neuroepithelial tumour grading based on the frequency domain techniques as well as be helpful in the selection of the brain tumour boundary. The HFP technique is recommended as part of MRI evaluations prior to brain tumour biopsy and removal.

Compliance with ethical standards

Guarantor The scientific guarantor of this publication is Lin Ma.

Conflict of interest The authors of this manuscript declare no relationships with any companies, whose products or services may be related to the subject matter of the article.

Funding This study has received funding from a Special Financial Grant from the China Postdoctoral Science Foundation (2014 T70960), the Foundation for Medical and Health Science and Technology Innovation Project of Sanya (2016YW37), National Natural Science Foundation of China (91520202) and Youth Innovation Promotion Association CAS.

Statistics and biometry One of the authors has significant statistical expertise.

Informed consent Written informed consent was not required for this study because this is a retrospective study, and MRI sequences and diffusion-weighted imaging are routinely performed in clinical practice at our hospital.

Ethical approval Institutional Review Board approval was obtained.

Methodology
• retrospective
• diagnostic or prognostic study
• performed at one institution

References

1. Louis DN, Ohgaki H, Wiestler OD, Cavenee WK, Burger PC, Jouvet A et al (2007) The 2007 WHO classification of tumours of the central nervous system. Acta Neuropathol 114:97–109
2. Watanabe M, Tanaka R, Takeda N (1992) Magnetic resonance imaging and histopathology of cerebral gliomas. Neuroradiology 34: 463–469
3. Felix R, Schorner W, Laniado M, Niendorf HP, Claussen C, Fiegler W et al (1985) Brain tumors: MR imaging with gadolinium-DTPA. Radiology 156:681–688
4. Law M, Yang S, Wang H, Babb JS, Johnson G, Cha S et al (2003) Glioma grading: sensitivity, specificity, and predictive values of perfusion MR imaging and proton MR spectroscopic imaging compared with conventional MR imaging. AJNR Am J Neuroradiol 24: 1989–1998
5. Chen WX, Lou HY, Zhang HP, Xiu N, Lan WX, Yang YX et al (2011) Grade classification of neuroepithelial tumors using high-resolution magic-angle spinning proton nuclear magnetic resonance spectroscopy and pattern recognition. Sci China Life Sci 54:606–616
6. Herminghaus S, Dierks T, Pilatus U, Möllerhartmann W, Wittsack J, Marquardt G et al (2003) Determination of histopathological tumor grade in neuroepithelial brain tumors by using spectral pattern analysis of in vivo spectroscopic data. J Neurosurg 98:74–81
7. Xiao HF, Chen ZY, Lou X, Wang YL, Gui QP, Wang Y et al (2015) Astrocytic tumour grading: a comparative study of three-dimensional pseudocontinuous arterial spin labelling, dynamic susceptibility contrast-enhanced perfusion-weighted imaging, and diffusion-weighted imaging. Eur Radiol 25:3423–3430
8. Di Costanzo A, Pollice S, Trojsi F, Giannatempo GM, Popolizio T, Canalis L et al (2008) Role of perfusion-weighted imaging at 3 Tesla in the assessment of malignancy of cerebral gliomas. Radiol Med 113:134–143
9. Yan XU, Chen Y, Wang F, Radiology DO (2013) Susceptibility weighted imaging in evaluating the histopathologic grade of cerebral neuroepithelial tumors. J Clin Radiol 32:1388–1393
10. Sakata A, Okada T, Yamamoto A, Kanagaki M, Fushimi Y, Dodo T et al (2015) Grading glial tumors with amide proton transfer MR imaging: different analytical approaches. J Neuro-Oncol 122:339–348
11. Price SJ, Fryer TD, Cleij MC, Dean AF, Joseph J, Salvador R et al (2009) Imaging regional variation of cellular proliferation in gliomas using 3'-deoxy-3'-[18F]fluorothymidine positron-emission tomography: an image-guided biopsy study. Clin Radiol 64:52–63
12. Tsuchida T, Takeuchi H, Okazawa H, Tsujikawa T, Fujibayashi Y (2008) Grading of brain glioma with 1-11C-acetate PET: comparison with 18F-FDG PET. Nucl Med Biol 35:171–176
13. Chen Z, Ma L, Lou X, Zhou Z (2010) Diagnostic value of minimum apparent diffusion coefficient values in prediction of neuroepithelial tumor grading. J Magn Reson Imaging 31:1331–1338
14. Shanbhag SS, Udupi GR, Patil M, Ranganath K (2013) A new method of analysing the intracerebral haemorrhage signal intensity on brain MRI images using frequency domain techniques. J Biomed Sci Eng 06:56–64
15. Torp SH (2002) Diagnostic and prognostic role of Ki67 immunostaining in human astrocytomas using four different antibodies. Clin Neuropathol 21:252–257
16. Metz CE (1986) ROC methodology in radiologic imaging. Investig Radiol 21:720–733
17. Doubilet PM (1988) Statistical techniques for medical decision making: applications to diagnostic radiology. AJR Am J Roentgenol 150:745–750
18. Park SH, Goo JM, Jo CH (2004) Receiver operating characteristic (ROC) curve: practical review for radiologists. Korean J Radiol 5: 11–18
19. Metz CE (2006) Receiver operating characteristic analysis: a tool for the quantitative evaluation of observer performance and imaging systems. J Am Coll Radiol 3:413–422
20. Shanbhag SS, Udupi GR, Patil KM, Ranganath K (2014) Quantitative analysis of diffusion weighted MR images of brain tumor using signal intensity gradient technique. J Med Eng 2014:1–8